CHAPTER 1

EXISTING INFORMATION ON TaS_2 SINGLE CRYSTALS

CONTENTS

1.1 Scope of the Present Work

TaS_2 (tantalum disulphide) belongs to a class of group V dichalcogenides having CdI_2 type structure. This compound has aroused much interest on account of its varying properties observed in the various forms : from semiconducting in the 1T-structure and superconducting in the 2H-form to a "mixture" of both in the recently discovered 4H(b) - TaS_2 type. The discovery of intercalation of these compounds by metals and organic molecules has further spurred a great deal of interest in them. Inspite of all this impertance, its mode of growth, etching behaviour, defect structure, etc. have not been studied so far.

Conditions for growing TaS_2 by direct vapour transport method have been worked out and surfaces of the as grown crystals have been examined to deduce the mechanism of growth of these crystals.

Since dislocations affect the physical properties of the crystals, it was considered worthwhile to reveal basal and non-basal dislocations in tantalum disulphide crystals. Etching technique has been used to study non-basal dislocations whereas basal dislocations have been investigated by transmission electron microscopy (TEM). TEM observations have been made by using bright field, dark field and weak beam techniques. Superiority of weak beam technique has been shown by giving elegant examples. Patterns obtained from using weak beam technique have also been used for the estimation of the stacking fault energy in TaS_2. Since electron microscope has provision for heating and cooling the specimens, studies of phase transformations in TaS_2 have been carried out in detail. Also a variation of lattice parameter 'a' with temperature has been studied for 2H-TaS_2 crystals.

The phenomenon of polytypism is well known for compounds having layered structures. A study of polytypism carried out during the course of present work has also been described. In addition electrical

and thermoelectrical properties have also been studied.

This chapter gives a general information on TaS_2 crystals.

1.2 Occurrence and Synthesis

TaS_2 is not known to occur naturally and so crystals have been grown in the laboratory by a chemical vapour transport method. A brief description of the various attempts made by earlier workers to grow these crystals have been given below.

Synthetically 1T-TaS_2 crystals were prepared with iodine as the transporter by Brouwer and Jellinek[1], Revelli and Phillips[2], Conrey and Pisharody[3] and Schafer et al.[4] with the aid of sulphur vapour. Temperature gradients differ slightly, $T_H = 950^\circ \rightarrow T_L = 900^\circ$ C[1] and $T_H = 970^\circ \rightarrow T_L = 750^\circ$C.[2]

Various ampoule sizes are reported ranging from 150 to 250 mm in length and 25 mm in diameter. The iodine concentration was 4 mg cm^{-3} tube volume, the reaction time about one week and yellow 1T-TaS_2 plates was the product.

Revelli and Phillips[2] succeeded in obtaining crystals of 2H-variety by prereacting the

elements in the presence of iodine at 950° C for several days followed by transport from T_H = 870° → T_L = 750° C in 10 days time.

Crystals of 3R-variety have not been reported in growth experiments. Crystals of 4H(b)-TaS_2 have been produced by Di Salvo and co-workers[5] by chemical transport with iodine as the transporter. The growth temperature reported is 700° C and the crystal size obtained is 4 x 4 x 2 mm^3.

The 6R-type was first obtained by Hagg and Schonberg[6] and called δ-TaS_2. Jellinek[7] produced the same type and determined it to be the 6R-form.

In Jellinek's batch, one sample which had been heated for a short time gave a diffraction pattern that could be indexed with a unit cell containing only $\frac{1}{3}$ TaS_2, and this had evidently a random layer structure (Random TaS_2 probably similar to that of $NiBr_2$ or $CdBr_2$). The preparation and growth techniques are summarised in Table 1.1. Some relevant data pertaining to TaS_2 are given in Table 1.2.

1.3 Crystal Structure

TaS_2 belongs to a CdI_2 structure (Fig. 1.1)

Table 1.1

Compound preparation and crystal growth techniques of TaS_2 single crystals

Compound preparation procedures	Ref.	Crystal growth techniques	Ref.
Direct synthesis at 600°, 800° or 1000° C, either annealed at 800 - 1000°C or homogenized, gives 2H-, 3R, 6R- and 1T-TaS_2. The 6R always mixed with 1T-form. Prolonged heating at 800° C yields increasing amount of 6R-TaS_2.	7	T_2 transport T_H= 1000° → T_L=800°C; 4 mg I_2 cm^{-3}, tubes 250 mm x 25 mm or 150 mm x 25 mm, period of 1-week, gives 2H-TaS_2. if SnS_2 is added, product is 2H- and 1T-TaS_2.	3
Direct synthesis at 900°C for 1-week	3	T_H= ? T_L= 700°C, gives 4Hb-TaS_2, nothing else is specified.	5
		T_H = 950° → T_L= 900° C ; rapid quenching nothing else specified.	1
Heating stoichiom. 2H-TaS_2 at 950°C under ~1 atm. S_2 press. for 24 h, air quenched, gives 1T-TaS_2 quenched from 950°C, without excess S, gives 4Hb + 1T + 6R.	5	T_H = 950° → T_L = 850°C, 1-week, iodine	10
		T_H = 870° → T_L = 750°C, in 10 days, nothing else specified.	2
Reaction of stoichiom. amounts of Ta and S at 900°C for days, slow cooling gives 2H-TaS_2 with slight excess S, and then water quenched, it yields 1T-TaS_2.	8,9	T_H = 900° → T_L = 700°C, with iodine,	11
		T_H = 925° → T_L = 725°C, with bromine, nothing else specified.	
		T_H = 800° → T_L = 700°C, with iodine	4
		T_L = 800° → T_H = 1000°C, with sulfur, tubes; 110 mm x 17 mm.	

Table 1.2

Some relevant data pertaining to TaS_2

(a)	Luster	High shining metallic
(b)	Colour	Pale yellow
(c)	X-ray density	6.69 gm. ml^{-1}.
(d)	Mol. wt.	490.15
(e)	Melting point	Greater than 1300° C.
(f)	Solvents	Slightly soluble in HF + HNO_3
(g)	Unit cell volume	60.811 $Å^3$
(h)	Cleavage planes	(0001)
(i)	Mol. per unit volume	One
(j)	Structure type	CdI_2
(k)	Character	Covalent
(l)	Group	V D_{3d}^3 - P $\bar{3}$m 1.
(m)	Structure	Trigonal prismatic layer structure

which has an hexagonal unit cell containing a single molecule, with cations at special positions (0, 0, 0) and anions at positions ($\frac{1}{3}$, $\frac{2}{3}$, u) and ($\frac{2}{3}$, $\frac{1}{3}$, -u) of space group $p\bar{3}m1$, where u is approximately $\frac{1}{4}$. Figure 1.2 gives a schematic view of TaS_2 lattice.

Each layer of TaS_2 is 3 atoms thick, the top and bottome sheets are sulphur and the middle sheet is tantalum (Fig. 1.3). The atomic sheets are all regularly close packed so the usual notation for hexagonally packed atoms may be used. An individual layer may have AbC or AbA stacking. (The capital letters refer to the sulphur and the lower letters to the tantalum atoms). In the AbC layers the tantalum atoms are at the centre of the sulphur octahedra while in the AbA layers they are at the centre of trigonal prism of sulphur (Fig. 1.4). The crystal structure is then obtained by stacking these octahedral and/or trigonal layers in an orderly way on top of one another. The ionic radius of Ta is 0.68 Å and that of S is 1.84 Å. The unit cell dimensions of known polytypes of TaS_2 are given in Table 1.3, and are schematically represented in Fig. 1.5. A detail study of polytypism carried out by the author is described in chapter 8.

Table 1.2

Known Polytypic Modifications of TaS_2

No.	Polytypes (Ramsdell notation)	Structure (Zhdanov notation)	Space group	Hexagonal unit cell dimensions		Reference
				a Å	c Å	
		Polytypes with known structures				
1.	1T	Octahedral	P $\bar{3}$ m	3.36	5.90	7
2.	2H	Trigon. Prism	$P6_3/mmc$	3.315	12.10	7
3.	4H	Trigon prism + octahedral	$P6_3/mmc$	3.332	23.62	1
4.	6R	Trigon prism + octahedral	R 3 m	3.335	35.85	7

In this group of layered compounds the bonding in one-slab is strong, the interlayer forces are weaker and this results in the atomic lattice of high anisotropy both mechanically and electrically with easy cleavage and extended growth perpendicular to the hexagonal/trigonal symmetry axis. The sandwiches themselves are strongly, partially covalent bonded. The interalayer forces are atleast one hundred times greater than the interlayer.[12)]

1.4 Intercalation

The main interest in intercalated materials lies in the fact that many of their crystallographic and electric properties make them promising systems in which to investigate mechanisms of superconductivity which may rely upon two-dimensional constraints. The effect of intercalation is to introduce into the Van der Waals gap alkali metal atoms or molecules of organic complexes which may modify their structural and electrical properties. Almost all layer compounds have the property of intercalating alkalies or organic materials, usually with the result that the molecular sandwiches of the lattice are pushed further apart.

The first account of intercalation in

layer compounds was by Rudorff[13] during a study of the take-up of alkali metals from liquid ammonia solution. Some of these compounds have since been shown to be superconducting. Intercalation tends to produce a material composition A_xMX_2 where x is fixed for a given MX_2, but is usually less than one. For example WS_2, MoS_2 and NbS_2 will intercalate potassium with x = 0.5, 0.6, 0.8 respectively. Both the a-axis and c-axis, but more particularly the c-axis, is increased in length by intercalation. The relative c-expansion is smaller as x increases, and suggests an increasing tendency towards ionic behaviour. The metal insulator transition in these compounds is such that metallic conduction does not appear until the alkali metal content is quite large.

Studies have been made of superconducting layer compounds intercalated with organic materials, e.g. pyridine, forming for example $NbS_2(Py)_{1/2}$[14] or $TaS_2(Py)_{1/2}$[15]. Studies of temperature dependence of electrical resistivity, Hall effect, and the magnetic susceptibility indicate that the crystallographic distortion apparent in metallic layer dichalcogenides at low temperatures is absent after intercalation.

Expansion of the lattice of TaS_2

intercalated with pyride may be followed directly by high resolution electronmicroscopy[16]. The interlayer spacing increases from 0.6 to 1.0 nm on intercalation.

At room temperature, resolutions of 2 Å to 3 Å were obtained in powders and crystals of 2H-TaS_2, 2H-TaS_2 $(C_5H_5N)_{1/2}$ and 2H-$TaS_2(C_5H_5N)_{1/4}$, under optimum conditions for direct imagining of the atomic lattice and related structural details. With the incident beam normal to the a-plane of thin TaS_2 crystals regular hexagonal moire patterns were seen as transmission images of overlaping layers of TaS_2 planes; this represents an incident resolution of the atomic array at 1 Å spacing.

In intercalated TaS_2 the spacing between the layers can vary from 3 Å to 30 Å, with little effect on the entropy associated with the superconducting specific heat anomaly[17] which must therefore arise mainly from two-dimensional correlations. Tracey et al.[18] have prepared intercalates between TaS_2 and $NbSe_2$ and a number of metals (e.g. Hg, Ga, In, Cd, Sn, Pb) and alloys, X-ray data for these are listed in Table 1.4.

1.5 Electrical Properties

In its 1T modification TaS_2 is a

Table 1.4

Intercalated Compounds Between TaS_2 and different metals[18)]

Compound	a_o A°	c_o A°	Reaction time (days)/ temp °C.
TaS_2	3.315	12.08	
TaS_2(Hg) red	3.325	9.058	4/200
TaS_2(Hg) bleak	3.325	8.923	5/200
$TaS_2(In)_{0.5}$	3.320	7.97	7/450
$TaS_2(Cd)_{0.9}$	3.311	17.44	4/550
Pure phase $TaS_2(Cd)_{0.9}$ Two phase mixture	3.311	13.58 } 17.44 }	5/550
$TaS_2(Sn;Cd)_x$	~3.32	6.7 x n	2/500
TaS_2(Sn;Cd; Bi;Pb)$_x$	3.3	6.68 x n 7.08 x n	5/450

material which is metallic at room temperature, but reverts to semi-conduction at low temperatures. The transition between the metallic state and the semi-conducting state has been studied as a function of temperature by Thomson et al.[10] The electrical properties of 1T-TaS_2 indicate two-phase transformations at temperatures of 190° K and 348° K. As the temperature increases between these limits the electrical resistivity decreases by an order of magnitude. The higher temperature transition is a semi-conductor-metallic transition through which the resistance decreases by a factor of two. A third transition exists at 315° K. Chu and Huang[19] find that the semi-conductor-metal transition is suppressed linearly by compression up to a pressure of about 15 K bars with $\Delta T_c/\Delta P = (3.0 \pm 0.2)$ K/k bar. A two band model with a small but temperature and pressure dependent overlap is required to explain these observations.

At liquid helium temperatures intercalated tantalum disulphide is a super-conductor, and diamagnetic anisotropy associated with the transition to the superconducting state is seen above 3.5° K.[20] The anisotropy grows inversely with temperature

obeying roughly a diamagnetic Curie Law. It seems plausible to ascribe it to electron correlations which at lower temperature are responsible for superconduction.

The Seebeck coefficient of 1T-TaS_2 changes sign from negative to positive on warming through the 352°K transition, whereas the Hall coefficient remains negative, only a break occurs. Above the upper transition the charge carriers suffer heavy scattering.

Resistivity anisotropies have been measured for 2H-TaS_2[15,21] and 4Hb-TaS_2[22,5]; the 4Hb-TaS_2 has metallic conduction along the layers but behaves like a semi-metal or semiconductor across the layers with a resistivity anisotropy as large as 500 at low temperatures. 2H-TaS_2 is metallic across the layers down to $\sim 70^\circ$K, and then, an increase in $\rho_\perp$ occurs. The pressure dependence of $\rho_\parallel$ has been measured for 1T-TaS_2[23, 19, 24]. The various anisotropies observed as well as the large pressure dependence suggest that electron mobility perpendicular to the layer is critically dependent on the interlayer interactions.

A summary of resistivity and Hall coefficient data on single crystals of TaS_2 is given

in Table 1.5.

1.6 Optical Properties

Spectra for the series of TaS_2 polytypes, 2H-4Hb -, and 1T- when considered, give the clearcut illustration of the effect of changes in local crystal field environment of the cation. The 2H polytype gives a density of states closely resembling that of 2H-$NbSe_2$, whilst the 4Hb polytype which consists of alternate layers of trigonal prismatically and octahedrally coordination sandwiches, gives a density of states which appears to be a linear average of those for the 2H- and 1T- structures, suggesting independent contributions from different types of layer. This again demonstrates the weak interlayer coupling experienced in the predominantly two dimensional materials. All these polytypes show considerable change in relative weighting of features in the density of states between He_I and He_{II}, as was also observed for HfS_2. Not only does the 'd' band intensity decrease relative to the rest of the bands at the lower photon energy as expected for the photon energy dependence of cross section for 'p' and 'd' states,

Table 1.5

A Summary of resistivity and Hall Coefficient data on TaS_2 single crystals

Structure	Resistivity			Hall coefficient			Reference
	$\rho_{\parallel}$ at room temp. ($\mu\Omega$ cm)	Temp. range measured (K)	Temp. at which anomalies occur	R at room temp. (10^{-4} cm^3/C)	Temp. range measured (K)	Temp. range in which it varies	
1T-TaS_2	$\sim$ 1000	4–400	$\sim$ 200 K 350 K	negative	-	-	25,26
2H-TaS_2	150 150[a]	4–300	75 K	+ 2.5	4–250	20–70	27,19
4Hb-TaS_2	390 $\pm$ 60	4–370	20 K 315 K	-	-	-	20

symbols : $\rho_{\parallel}$ resistivity in a direction parallel to the crystal layers.
R Hall coefficient.

but considerable intensity changes also occur within the 'p' band. For 1T-TaS_2 in particular, the prominent state 2.5 eV below E_f at He_I is almost absent in the He_{II} spectrum.

The interchange in intensity between 'p' and 'd' like features in the valence band as the photon energy is varied has been beautifully illustrated by Eastman in recent photoemission measurements from 2H-TaS_2 employing monochromated synchrotron radiation as the excitation source.[28)]

Elegant angular photoemission studies of the group V_a dichalcogenides 1T-TaS_2 and 1T-$TaSe_2$ have recently been reported by Smith and co-workers.[29-31)]

The 1T form of TaS_2 exhibits an infrared reflectivity with some metallic characteristics in its high temperature phase.

1.7 Uses

The dichalcogenides of tantalum have received considerable attention in the recent years on account of their special uses in the areas of thermoelectricity, superconductivity and also lubrication.

1.8 References

1. Brouwer, R., and Jellinek, F.
Mat. Res. Bull. 9 (1974) 827.

2. Revelli, J. F., and Phillips, W. A.
J. Sol. Stat. Chem. 9 (1974) 176.

3. Conrey, L. E., and Pisharody, K. P.
J. Sol. State. Chem. 4 (1972) 345.

4. Schafer, H., Wehmeier, F., and Trenkel, M.
J. Less Comm. Metals 16 (1968) 290.

5. Di Salvo, F. J., Bagley, B. G., Voorhoeve, J. M., and Waszczak, J. V.
J. Phys. Chem. Sol. 34 (1973) 1357.

6. Hagg, G., and Schonberg, N.
Arvik Kemi. 7 (1954) 371.

7. Jellinek, F.
J. Less Comm. Metals 4 (1962) 9.

8. Gamble, F. R., and Thomson, A. H.
Private Communication.

9. Gamble, F. R., Di Salvo, F. J., Klemm, R. A., and Geballe, T. H.
Science 168 (1970) 568.

10. Thomsen, A. H., Gamble, F. R., and Revelli, J.F.
Sol. Stat. Comm. 9 (1971) 981.

11. Van Maaren, M. H., and Schaffer, G. M.
Phys. Lett. 24 A (1967) 645

12. Verble, J. L., and Wietling, T. J.
Solid Stat. Comm. 11 (1972) 941.

13. Rudorff, W.
Chimia 19 (1965) 489.

14. Ehrenfreund, E., and Gossard, A. C.
Phys. Rev. B 5 (1972) 1708.

15. Thomsen, A. H., Gamble, F. R.
and Koehler, R. F.
Phys. Rev. B 5 (1972) 2811.

16. Thomas, J. M., Evans, E. L.,
Barch, B., and Jenkins, J. L. L.
Nature (Phys. Sci.) 235 (1972) 126.

17. Di Salvo, F. J., Schwall, R.,
Geballe, T. H., Gamble, F. R., and
Osaiki, J. H.
Phys. Rev. Letters 27 (1971) 310.

18. Tracey, T., Gentile, P. S. and
Budnik, J. T.
O.N.R. Conference on the Physics and
Chemistry of layer compounds,
Monterey, California, U.S.A. 1972,
Conference Abstracts.

19. Chu, C. W., and Huang, S.
Phys. Letters 36 A (1971) 93.

20. Geballe, T. H., Menth, A., Di Salvo, F.J.,
and [illegible], Gamble, F. R.
Phys. Rev. Letters 27 (1971) 314.

21. Tidman, J. P., Singh, O., Curzon, A. E.,
and Frindt, R. F.
Phil. Mag. 30 (1974) 1191.

22. Tidman, J. P., and Frindt, R. F.
unpublished.

23. Di Salvo, F. J., Maines, R. G.,
Waszczak, J. V., and Schwall, R. E.
Solid State Commun. 14 (1974) 497.

24. Grant, A. J., Griffiths, T. M., Pitt, G. D., and Yoffe, A. D.
Int. Conf. on Physics of Semiconductors, Stuffgart.

25. Tubbs, M. R.,
Phys. Stat. Solidi 49 (1972) 1.

26. Wilson, J. A., and Yoffe, M. D.
Adv. Phys. 18 (1969) 193.

27. Hahn, G., and Schonberg, N.
Arkiv fur Kemi. 7 (1954) 371.

28. Eastman, D. E.
Vacuum Ultra Violet Radiation Physics, Pergamon/Vieweg, Oxford/ Braunschweig, (1974) 417.

29. Smith, N. V., and Traum, M. M.
Phys. Rev. Letters 31 (1973) 1247.

30. Smith, N. V., Traum, M. M., and Di Salvo, F. J.
Sol. Stat. Commun. 15 (1974) 211.

31. Traum, M. M., Smith, N. V., and Di Salvo, F. J.
Phys. Rev. Letters 32 (1974) 1241.

Captions of the figures

Figure 1.1 Cadmium iodide layer structure. Small circles Cd, large circles I.

Figure 1.2 The basal plane and the stacking arrangement in the hexagonal unit cell.

Figure 1.3 Method of stacking of the layers in TaS_2.

Figure 1.4 Trigonal prism, stacking sequence AbA and octahedron, stacking sequence AbC.

Figure 1.5 Sections through the $(11\bar{2}0)$ planes of tantalum disulphide.

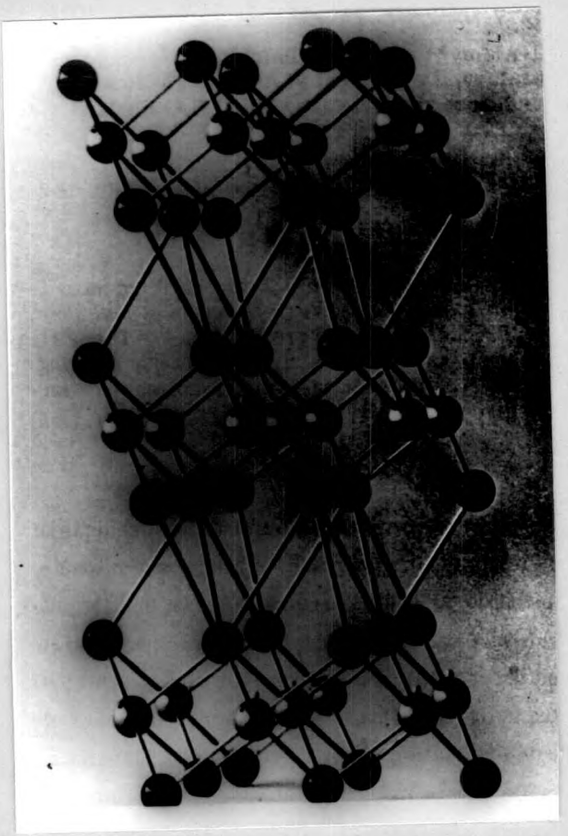

Fig. 1.1

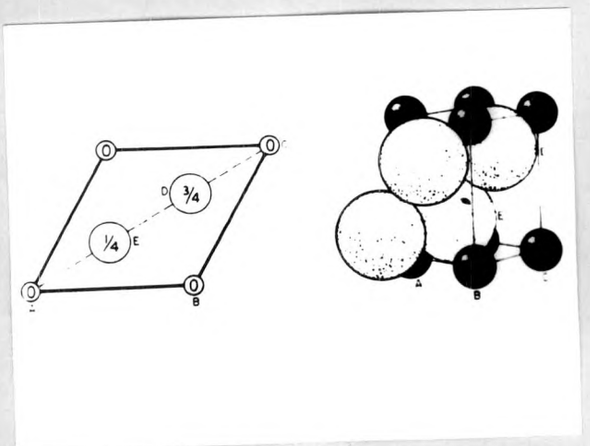

Fig. 1.2

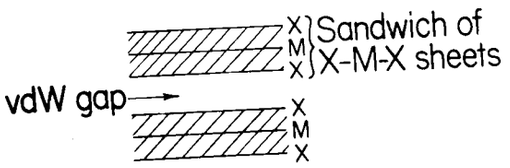

Fig. 1.3

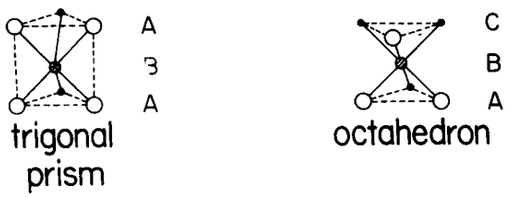

Fig. 1.4

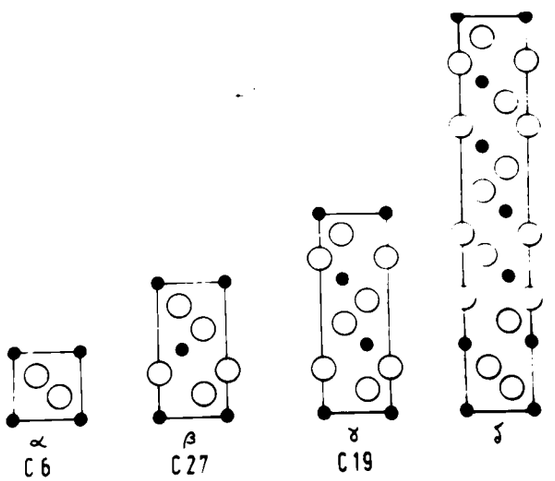

Fig. 1.5